Bull Volcanol (1989) 51:28–40

Bulletin of
Volcanology

The intensity of plinian eruptions

Steven Carey and Haraldur Sigurdsson

Graduate School of Oceanography, University of Rhode Island, Narragansett, RI 02882, USA
February 1988

Abstract. Peak intensities (magma discharge rate) of 45 Pleistocene and Holocene plinian eruptions have been inferred from lithic dispersal patterns by using a theoretical model of pyroclast fallout from eruption columns. Values range over three orders of magnitude from 1.6×10^6 to 1.1×10^9 kg/s. Magnitudes (total erupted mass) also vary over about three orders of magnitude from 2.0×10^{11} to 6.8×10^{14} kg and include several large ignimbrite-forming events with associated caldera formation. Intensity is found to be positively correlated with the magnitude when total erupted mass (tephra fall, surges and pyroclastic flows) is considered. Initial plinian fall phases with intensities in excess of 2.0×10^8 kg/s typically herald the onset of major pyroclastic flow generation and subsequent caldera collapse. During eruptions of large magnitude, the transition to pyroclastic flows is likely to be the result of high intensity, whereas the generation of pyroclastic flows in small magnitude eruptions may occur more often by reduction of magmatic volatile content or some transient change in magma properties.

The correlation between plinian fall intensity and total magnitude suggests that the rate of magma discharge is related to the size of the chamber being tapped. A simple model is presented to account for the variation in intensity by progressive enlargement of conduits and vents and excess pressure at the chamber roof caused by buoyant forces acting on the chamber as it resides in the crust. Both processes are fundamentally linked to the absolute size of the pre-eruption reservoir. The data suggest that sustained eruption column heights (i.e. magma discharge rates) are indicators of eventual eruption magnitude, and perhaps eruptive style, and thus are key parameters to monitor in order to assess the temporal evolution of plinian eruptions.

Introduction

Plinian eruptions are sustained, high-energy explosive discharges of magma that generate large convective plumes in the atmosphere and result in widespread tephra fallout over hundreds or thousands of square kilometres (Walker 1980, 1981a). The well-known eruption of Vesuvius which buried the cities of Pompei and Herculaneum in A.D. 79 (Lirer et al. 1973; Sigurdsson et al. 1985; Carey and Sigurdsson 1987) is the type-example of this kind of activity, although it is by no means the largest plinian event (Walker 1981a). The frequency of true plinian eruptions is such that only a few have occurred in the historic period during which reliable observations and measurements could be carried out. Deposits left by such eruptions are, however, common in the geologic record and preserve valuable information about the dynamics of these events.

Walker (1980) has proposed that five parameters are necessary to adequately characterize the nature of individual explosive eruptions: *intensity* is the rate at which magma is discharged; *magnitude* is the total mass of material erupted; *dispersive power* is the area over which the products are spread; *violence* refers to the distribution of products mainly by momentum; and *destructive potential* is an assessment of the area over which destruction of buildings, farmland and vegetation occurs. Two of these parameters, dispersive power and intensity, are closely related because the height of an eruption column, and thus its dis-

Offprint requests to: H Sigurdsson

persal power, is a direct function of magma discharge rate (Wilson et al. 1978; Settle 1978; Wilson et al. 1980; Sparks 1986; Carey and Sparks 1986). Furthermore, it has been suggested on theoretical grounds that eruption intensity is a key factor in determining the behaviour, i.e. convective rise or collapse, of an eruption column (Sparks and Wilson 1976; Sparks et al. 1978). The intensity of an eruption thus determines both the height to which material is injected into the atmosphere and the sequential development of eruptive phases (fallout, surge or flow generation). The importance of eruption intensity has been recognized by Fedotov (1985), who proposed a new scale for explosive eruptions based on a logarithmic index of magma discharge rate, similar to the Richter scale used for describing the magnitude of earthquakes.

In this paper we focus on the variation and controlling factors of intensity during plinian eruptions. The intensities of 45 well-documented plinian eruptions of Pleistocene and Recent age have been determined by using a theoretical model of pyroclast dispersal. Correlations of eruption intensity with other measurements of eruption bigness (Walker 1980) or scale, as we prefer, are tested to see if differences exist between eruptions of varying magnitude. We also examine the relationship between eruption intensity and the transitions of eruptive style (i.e. plinian fallout to pyroclastic flow generation) in the context of theoretical models for the stability of convective columns (Sparks and Wilson 1976; Sparks et al. 1978).

Determination of eruption intensity and magnitude

The dispersal of pyroclasts is controlled by a combination of eruption column height and transport by local winds and thus contains a component of eruption intensity. Carey and Sparks (1986) have developed a model of pyroclast dispersal which allow these two factors to be discriminated based on the geometry of particle isopleth maps constructed from field measurements. By using the model it is possible to calculate eruption column height and from that, eruption intensity based on the behaviour of convective plumes under a variety of atmospheric conditions (Sparks 1986). We estimate that the uncertainties in the column height and eruption intensity determinations are about ± 10–20%.

We have compiled data on 45 plinian eruptions of Pleistocene to Recent age for which intensities can be determined from published isopleth maps (Table 1). In all cases we use maximum lithic dispersal maps to avoid problems associated with pumice breakage during impact. Intensities calculated by this method represent the peak rate during an event. Although intensity is likely to vary during the course of an eruption, as shown, for example, by the A.D. 79 eruption of Vesuvius (Carey and Sigurdsson 1987), we feel that peak intensity is a useful way to characterize individual events.

The magnitude, or the total mass of material ejected, was also compiled for each eruption. In general, volume determinations of plinian deposits are subject to many uncertainties because limited preservation of the distal fine ash requires some type of extrapolation procedure. We have adopted the technique of Walker (1981a) which extrapolates a plot of isopach area versus thickness in order that the various deposits can be compared in a consistent manner. In addition, we have estimated the magnitude of both the plinian fallout phase and the total eruption in cases where pyroclastic flows and surges were produced (Table 1). The uncertainty associated with the total magnitude estimate may be as high as a factor of 2 because of post-eruptive erosion of pyroclastic deposits, the variable quality of field mapping, and uncertainties in estimates of the mass of fine distal ash.

Variations of intensity and magnitude

Inferred intensities of the 45 plinian eruptions vary from 1.6×10^6 kg/s to 1.1×10^9 kg/s. The highest intensity event was the Taupo ultraplinian eruption in New Zealand (Walker 1980), whereas the Shingo eruption of Towada volcano in Japan (Hayakawa 1985) was the lowest. Most of the eruptions tend to cluster in the intensity range of 2.5×10^7 to 2.5×10^8 kg/s, or within about one order of magnitude.

Magnitudes of the eruptions (fall, flow and surge combined) vary over a range of about three orders of magnitude from 2.0×10^{11} to 6.8×10^{14} kg. The largest-magnitude event was associated with the formation of the Atitlan caldera in Guatemala about 85 000 years ago. At the low end of the magnitude scale was the Oguni eruption of Towada volcano in Japan. A smaller range of magnitudes is found for the plinian fall phases alone (exclusive of pyroclastic flows and surges)

Table 1. Eruptive Parameters of Late Quaternary to Recent Plinian Eruptions

Eruption	Country	Date	Composition	Col. Ht.	MDR (kg/s)	DRE (km^3)	Plin. Mass (kg)	Time (h)	PF+S (DRE)	PF+S Mass	Total Mass	Reference
Toluca (lower)	Mexico	24500 YBP	And./Dac.	28	7.90E+07	0.4	9.0E+11	3.2	N.R.	N.R.	9.0E+11	Bloomfield et al. (1977)
Toluca (upper)	Mexico	11600 YBP	And./Dac.	30	1.00E+08	3.6	9.0E+12	25.0	N.R.	N.R.	9.0E+12	Bloomfield et al. (1977)
La Primavera B	Mexico	95000 YBP	Rhyolite	36	2.20E+08	16.0	4.0E+13	50.5	18.50	4.63E+13	8.6E+13	Walker et al. (1981) Wright (1981)
La Primavera D	Mexico	<95000 YBP	Rhyolite	26	7.90E+07	0.6	1.6E+12	5.6	N.R.	N.R.	1.6E+12	Walker et al. (1981) Wright (1981)
La Primavera E	Mexico	<95000 YPP	Rhyolite	24	6.30E+07	0.8	2.1E+12	9.1	N.R.	N.R.	2.1E+12	Walker et al. (1981) Wright (1981)
La Primavera J	Mexico	<95000 YBP	Rhyolite	33	1.80E+08	3.8	9.5E+12	14.7	N.R.	N.R.	9.5E+12	Walker et al. (1981) Wright (1981)
El Chichon A	Mexico	1982	Trachyand.	27	8.00E+07	0.3	7.5E+11	2.6	N.R.	N.R.	7.5E+11	Carey and Sigurdsson (1986)
El Chichon B	Mexico	1982	Trachyand.	32	1.50E+08	0.4	9.8E+11	1.8	0.13	3.2E+11	1.3E+12	Carey and Sigurdsson (1986)
El Chichon C	Mexico	1982	Trachyand.	29	8.50E+07	0.4	1.0E+12	3.3	N.R.	N.R.	1.0E+12	Carey and Sigurdsson (1986)
Santa Maria	Guatemala	1902	Dacite	34	1.70E+08	8.6	2.2E+13	35.1	N.R.	N.R.	2.2E+13	Williams and Self (1983)
Los Chocoyos	Guatemala	85000 YBP	Rhyodacite	45	5.00E+08	150.0	3.8E+14	208.3	120.00	3.00E+14	6.8E+14	Rose et al. (1987)
Apoyo A	Nicaragua	23000 YBP	Dacite	27	8.30E+07	2.8	7.0E+12	23.4	3.30	8.25E+12	1.5E+13	Sussman (1985)
Apoyo C	Nicaragua	<23000 YBP	Dacite	29	8.70E+07	2.5	6.3E+12	20.0	N.R.	N.R.	6.3E+12	Sussman (1985)
Nevado del Ruiz	Colombia	1985	And./Dac.	27	5.00E+07	<0.1	3.5E+10	0.2	0.004	1.00E+10	4.5E+10	Naranjo et al. (1986)
Pelee P1	Martinique	650 YBP	Rhyodacite	21	3.20E+07	0.1	2.0E+11	1.7	0.080	2.00E+11	4.0E+11	Traineau and Westercamp (1985)
Pelee P2	Martinique	1670 YBP	Rhyodacite	20	3.10E+07	0.1	2.0E+11	1.8	0.080	2.00E+11	4.0E+11	Traineau and Westercamp (1985)
Pelee P2	Martinique	2010 YBP	Rhyodacite	22	3.20E+07	0.1	2.0E+11	1.7	0.080	2.00E+11	4.0E+11	Traineau and Westercamp (1985)
Mount St. Helens	United States	1980	Dacite	19	1.90E+07	0.3	6.3E+11	9.1	0.03	8.88E+10	7.1E+11	Carey and Sigurdsson (1985)
Katmai	United States	1912	Rhy./Dac.	32	1.70E+08	3.5	8.8E+12	14.4	6.50	1.63E+13	2.5E+13	Fierstein and Hildreth (1986)
Askja	Iceland	1875	Rhyolite	26	7.90E+07	0.3	8.0E+11	2.8	0.03	8.88E+10	8.9E+11	Sparks et al. (1981)
Fogo	Azores	1563	Trachyte	19	1.90E+07	0.4	1.1E+12	15.4	N.R.	N.R.	1.1E+12	Walker and Croasdale (1973)
Fogo A	Azores	4600 YBP	Trachyte	30	1.00E+08	1.7	4.3E+12	12.0	N.R.	N.R.	4.3E+12	Walker and Croasdale (1973)
Vesuvius	Italy	A.D. 79	Phonolite	32	1.50E+08	2.1	5.1E+12	9.5	0.37	9.25E+11	6.1E+12	Sigurdsson et al. (1985)
Avellino	Italy	3500 YBP	Phonolite	30	1.00E+08	0.7	1.7E+12	4.7	N.R.	N.R.	2.0E+12	Pescatore et al. (1987)
Campanian Tuff	Italy	36000 YBP	Trachyte	44	3.20E+08	N.R.	N.R.		N.R.	N.R.	2.7E+14	Sigurdsson and Carey (unpublished) Cornell et al. (1983)

Santorini	Greece	1470 B.C.	Rhyolite	36	2.50E+08	N.R.	N.R.		N.R.	N.R.	3.3E+13	Watkins et al. (1978) Bond and Sparks (1976)
Tarawera	New Zealand	1886	Basalt	34	1.80E+08	0.7	1.8E+12	2.7	N.R.	N.R.	1.8E+12	Walker et al. (1984)
Hatepe	New Zealand	1820 YBP	Rhyolite	33	1.80E+08	1.5	3.8E+12	5.8	N.R.	N.R.	3.8E+12	Walker (1981b)
Taupo	New Zealand	1820 YBP	Rhyolite	51	1.10E+09	5.8	1.5E+13	3.7	25.00	6.25E+13	7.7E+13	Walker (1980)
Waimihia	New Zealand	3500 YBP	Rhyolite	42	3.70E+08	7.1	1.8E+13	13.3	N.R.	N.R.	1.8E+13	Walker (1981b)
Tambora (lower)	Indonesia	1815	Trachyand.	33	1.50E+08	0.5	1.2E+12	2.1	N.R.	N.R.	1.2E+12	Sigurdsson and Carey (in press)
Tambora (upper)	Indonesia	1815	Trachyand.	44	3.80E+08	1.2	3.0E+12	2.2	48.50	1.21E+14	1.2E+14	Sigurdsson and Carey (in press)
Oyu 1	Japan	1250 YBP	Dacite	30	1.00E+08	0.2	5.3E+11	1.5	2.00	4.50E+12	5.0E+12	Hayakawa (1985)
Mayogatai	Japan	3000 YBP	Dacite	19	1.90E+07	<0.1	9.0E+10	1.3	N.R.	N.R.	9.0E+10	Hayakawa (1985)
Chuseri	Japan	5400 YBP	Dacite	29	9.50E+07	1.7	4.0E+12	11.7	N.R.	N.R.	4.0E+12	Hayakawa (1985)
Oguni	Japan	7000 YBP	Dacite	16	9.00E+06	0.1	2.0E+11	6.2	N.R.	N.R.	2.0E+11	Hayakawa (1985)
Nambu	Japan	8500 YBP	Dacite	25	6.00E+07	0.4	9.7E+11	4.5	N.R.	N.R.	9.7E+11	Hayakawa (1985)
Natsuzaka	Japan	9500 YBP	Andesite	23	3.55E+07	0.3	5.7E+11	4.5	N.R.	N.R.	5.7E+11	Hayakawa (1985)
Shingo	Japan	10500 YBP	Dacite	12	1.58E+06	0.1	2.5E+11	44.0	N.R.	N.R.	2.5E+11	Hayakawa (1985)
Hachinohe 6	Japan	13000 YBP	Dacite	33	1.31E+08	0.7	1.6E+12	3.4	17.30	4.00E+13	4.2E+13	Hayakawa (1985)
Hachinohe 4	Japan	13000 YBP	Dacite	37	2.20E+08	0.4	8.6E+11	1.1	17.30	4.00E+13	4.1E+13	Hayakawa (1985)
Hachinohe 2	Japan	13000 YBP	Dacite	21	3.16E+07	0.1	2.1E+11	1.8	N.R.	N.R.	2.1E+11	Hayakawa (1985)
Maito 1	Japan	17000 YBP	Dacite	13	1.65E+06	<0.1	5.0E+10	8.4	N.R.	N.R.	5.0E+10	Hayakawa (1985)
Osumi	Japan	22000 YBP	Rhyodacite	44	4.17E+08	34.3	7.9E+13	52.5	150.00	3.45E+14	4.2E+14	Aramaki (1984) Kobayashi et al. (1983)
Shikotsu	Japan	20000 YBP	Rhyolite	39	3.16E+08	35.0	8.1E+13	70.8	45.00	1.04E+14	1.9E+14	Katsui (1959)

Key to column headings. Col. Ht. = inferred eruption column height in kilometres above the volcano, *MDR (kg/s)* = inferred magma discharge rate in kilograms per second, *DRE (km³)* = volume of plinian fall deposit expressed in cubic kilometres of magma (dense rock equivalent, density of 2500 kg/m³), *Plin. Mass (kg)* = mass of plinian fall deposit in kilograms, *Time (h)* = inferred duration of plinian fall in hours, *PF+S (DRE)* = volume of pyroclastic flows and surges expressed in cubic kilometres of magma (dense rock equivalent, density of 2500 kg/m³), *PF+S Mass* = mass of pyroclastic flow and surge deposits in kilograms, *Total Mass* = mass of fall, surge and pyroclastic flow deposits combined in kilograms, *N.R.* = not reported. *DRE (km³)* was calculated from tephra volume using reported bulk deposit densities and a magma density of 2500 kg/m³. In cases where bulk deposit density was not reported, a value of 800 kg/m³ was assumed for the entire fall deposit. *Plin Mass (kg)* was calculated from *DRE (km³)* using a magma density of 2500 kg/m³. *PF+S (DRE)* was calculated from tephra volume assuming a 1250 kg/m³ bulk deposit density and a magma density of 2500 kg/m³

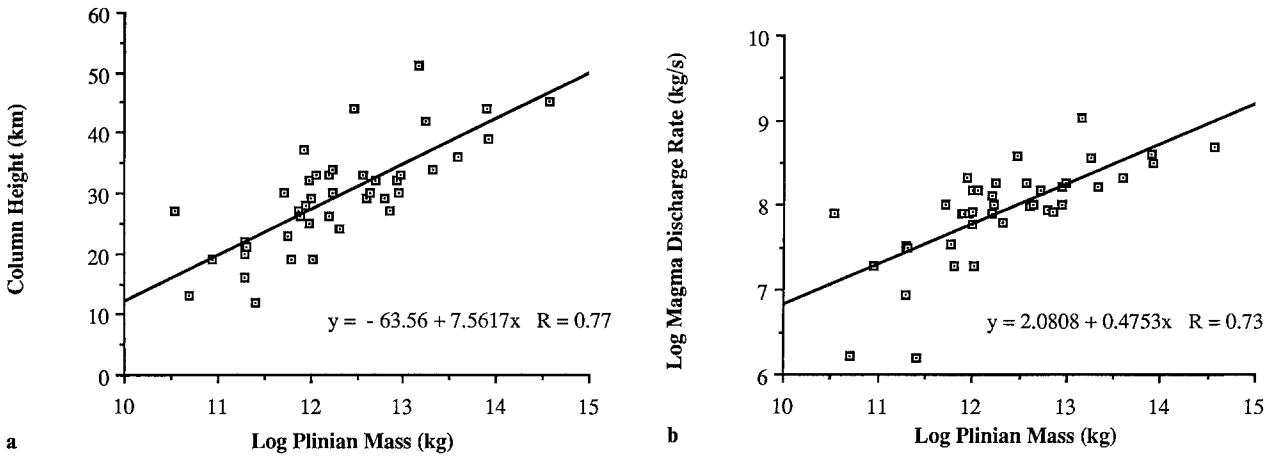

Fig. 1. a Eruption column height versus the log of the plinian fall deposit mass for Pleistocene and Recent plinian eruptions. The Campanian Tuff and Santorini eruptions (Table 1) are not included because separate estimates of the plinian fallout mass are not available. Column heights were calculated using the equations in Sparks (1986); **b** Log of the magma discharge rate (intensity) versus the log of the plinian fall deposit mass for Pleistocene and Recent plinian deposits. Magma discharge rates were calculated from the model of Carey and Sparks (1986). Both column height and magma discharge rate show a positive correlation with the mass of material erupted during the plinian fall phase

with values between 2.0×10^{11} and 8.0×10^{13} kg (Table 1). The type-example of plinian events, the 79 A.D. eruption of Vesuvius, falls in the middle of the observed range of magnitudes and intensities.

In their analysis of the A.D. 186 Taupo eruption of New Zealand, Wilson and Walker (1985) noted a crude positive correlation between the volume and intensity of various eruptive phases but offered no detailed explanation of its significance. Hayakawa (1985) also noted a correlation between the cross-wind width of lithic isopleths and the mass of some plinian deposits in Japan. He suggested that "eruption columns with a larger mass output reach higher elevations than smaller ones". These observations motivated us to test for such a relationship in a larger data set of eruptions (Table 1) and with intensity measurements that were consistently determined and better constrained by the use of pyroclast dispersal modelling. We find a similar positive correlation for the 45 eruptions between column height (Fig. 1a) or intensity (Fig. 1b) and the mass ejected during the plinian phase (magnitude). This correlation is significantly improved, however, if column height or intensity is plotted against the total erupted mass instead of just that produced during the plinian phase (Fig. 2a, b). Although the correlation exhibits considerable scatter ($r = 0.87$), it is quite clear that the highest *intensity* plinian phases are associated with eruptions of the largest *magnitude*.

Some eruptions deviate significantly from this relationship. A case in point being the 1985 eruption of Nevado del Ruiz in Colombia which had a relatively high intensity but a very low magnitude. This eruption was short-lived and produced a small deposit (Naranjo et al. 1986), thus the intensity was not sustained. The high column height was probably associated with a large instantaneous release of energy, in which case the model of sustained particle fallout is not applicable. Other eruptions which have created high, transient eruption columns in response to "instantaneous" discharges of energy include the May 18, 1980 eruption of Mount St. Helens (Sparks et al. 1986) and probably the 1956 eruption of Bezymianny (Gorschkov 1959).

Of the eruptions that were unequivocally sustained plinian events, those with intensities greater than about 2.0×10^8 kg/s were associated with caldera formation and the emplacement of major ignimbrites with volumes typically exceeding 15 km^3 (DRE). Some of the intermediate magnitude events are also associated with small caldera formation but as the magnitude decreases, the nature of the activity changes to predominantly central-vent stratovolcano eruptions with some pyroclastic flows and surges but no major collapse structures.

Factors controlling the intensity of plinian eruptions

The observed correlation between intensity and magnitude suggests that the peak intensity of a

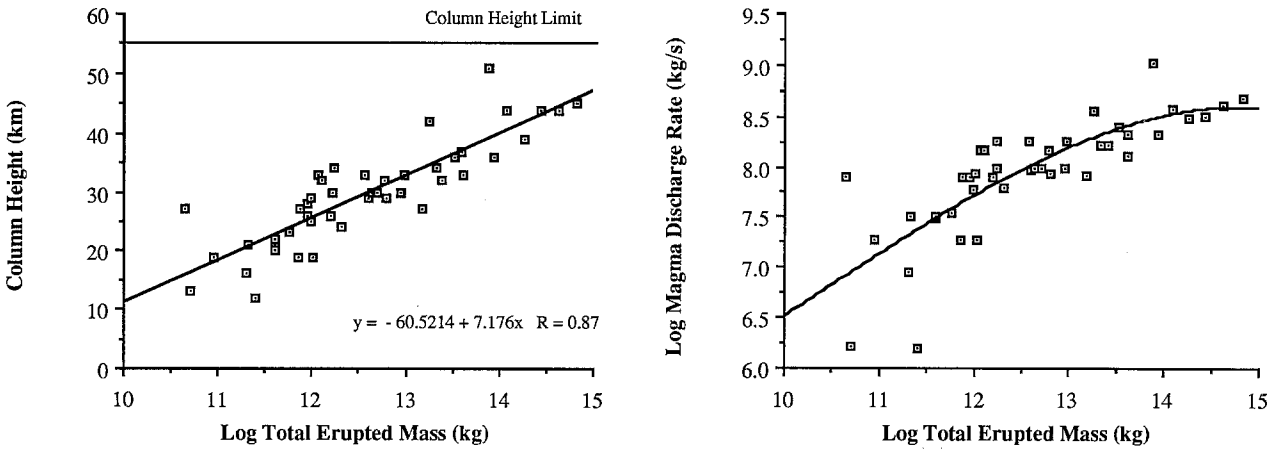

Fig. 2. a Eruption column height versus the log of the total erupted mass for Pleistocene and Recent plinian eruptions. Total erupted mass includes fall, surge and pyroclastic flow deposits. *Inclined solid line* is a linear regression of the data with the equation shown in the box. *R* is the correlation coefficient of the regression. The *solid horizontal line* is the upper theoretical limit of sustained eruption column height from Wilson et al. (1978); **b** Log of the magma discharge rate versus total erupted mass for late Quaternary and Recent plinian eruptions. Note the improved correlation of *a)* and *b)* compared to similar plots in Fig. 1 involving only the mass of material erupted during the plinian fall phase

plinian eruptive phase is related to the total mass of material that will be erupted during a continuous eruptive sequence. This relationship immediately raises the question of why the total volume of magma discharged during an explosive eruption should control the rate at which magma is discharged during its plinian phase. The intensity of a plinian eruption is governed primarily by the pressure gradient between the magma chamber and the surface, the viscosity and volatile content of the magma, and the dimensions of the conduit.

Pressure gradients

Wilson et al. (1980) and Wilson and Head (1981) have assumed that the pressure gradient below the level where vesiculation occurs, results from the difference between the hydrostatic head of the magma column and the lithospheric pressure in the surrounding crustal rocks. It is likely, however, that other pressure terms are important at the inception of an eruption.

Establishment of crustal magma chambers occurs when buoyant uprise of melt is inhibited by increasingly brittle, lower-temperature, lower-density, upper crustal rocks (Elder 1979a, 1979b). Eruptions occur as the system attempts to establish isostatic equilibrium by fracturing a path to the surface for magma discharge. A combination of the magmatic pressure, local stress field, and the tensile strength of the chamber cap will determine the geometry of the magma pathways and the critical conditions of formation (e.g. Robson and Barr 1964; Pollard and Muller 1976; Shaw 1980). Whitney and Stormer (1986) point out that prior to eruption, buoyant forces act on magma reservoirs because underlying regions that have been heated by the passage of melt are sufficiently deformable to transmit the local lithostatic pressure to the base of the reservoir. Because the magma is a fluid, this pressure is exerted on the reservoir roof and is higher than the local lithostatic pressure by an amount:

$$P = 98.0655 \int \Delta\partial \, dL \qquad (1)$$

where P is pressure in bars and the integral is evaluated over the vertical extent of the chamber (L in km), and $\Delta\partial$ is the density contrast between magma and crustal rocks in g/cm^3. In other words, the excess pressure at the chamber roof is the buoyant force acting on the chamber in a 'fluid' of crustal density. Weertman (1971) identified this as the Peach-Koehler force in his analysis of a fluid-filled crack contained within a solid and stated that it is identical in magnitude to the Archimedian buoyancy force on a solid within a liquid. The amplitude of this force can be seen by inspection of equation (1) to be a function of chamber size.

The implication of equation (1) is that significant magma overpressure can occur in large chambers and that the magnitude of the initial pressure gradient should be a function of chamber size and density contrast between magma and country rock. Consider a magma chamber at some

depth D in the crust which has a vertical extent L. The pressure gradient at the onset of an eruption will be the result of: (1) the difference between the change in pressure within the magma column relative to the change in lithospheric pressure as given by $g\Delta\partial$, where g is the acceleration due to gravity and $\Delta\partial$ is the density contrast between magma and crustal rocks (Wilson and Head 1981) and (2) the pressure derived from the buoyant force acting on the chamber, as given in expression (1), divided by the distance from the top of the chamber to the surface. Combining these two components results in an expression for the total pressure gradient P_g as:

$$P_g = g\Delta\partial\left[\frac{1+L}{D}\right] \quad (2)$$

The total pressure gradient is thus related to the density contrast between magma and crust, the vertical extent of the chamber and the depth of the chamber. For a chamber of constant size, the initial pressure increases if the resides at shallower levels in the crust. Figure 3 illustrates the values of initial pressure gradient as a function of vertical chamber extent for a series of reservoirs at various depths. At a constant depth the gradient increases monotonically with increasing chamber size. Chambers of about 6 km vertical extent are associated with pressures similar to the tensile strength of crustal rocks.

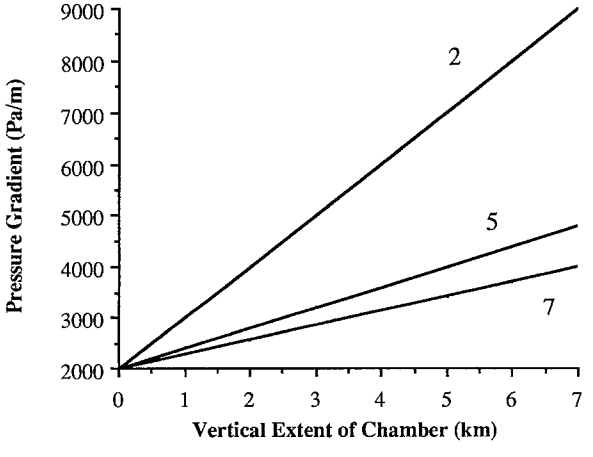

Fig. 3. Variation in initial pressure gradient as a function of vertical magma chamber extent for reservoirs at 2, 5, and 7 km depth in the crust. The density difference between magma and crust was taken as 200 kg/m^3

Volatile content

The effect of volatile content on magma discharge has been considered on a theoretical basis by Wilson et al. (1980) and Wilson (1980). These studies have suggested that intensity is only weakly dependent on magmatic volatile content. Volatile content does, however, have a more pronounced effect on the exit velocity of clasts at the vent and thus will govern the ballistic emplacement of clasts in proximal areas. Changes in volatile content during an eruption are unlikely to be recorded in distal plinian fall deposits because widespread dispersal of clasts is more strongly governed by convective velocities within the plume, which in turn are a function primarily of mass eruption rate (Wilson et al. 1978; Wilson et al. 1980).

Conduit dimensions

The dimensions of the pathways which magma takes from crustal chambers to the surface will be critical to the intensity of an eruption. This can be demonstrated by considering the equation presented by Wilson et al. (1980) for the mass eruption rate at the level below gas exsolution:

$$M = \frac{\pi r^4 g\partial_m(\partial_{cr}-\partial_m)}{8n} \quad (3)$$

where M is the mass eruption rate, r the conduit radius, g the acceleration due to gravity, ∂_m the magma density, ∂_{cr} the crustal density and n is the magma viscosity. The mass eruption rate varies as the fourth power of the conduit radius and therefore the roughly three order of magnitude range inferred from the intensity modelling could be accomodated by a change in r of only a factor of 6. Of course, equation (3) only applies below the level of vapour exsolution. In the upper portions of the conduit, vapour exsolution and fragmentation increases and then drastically reduces the viscosity of the erupting mixture. For many eruptions, however, the distance travelled below the exsolution level is greater than above, and integration over the whole vertical interval yields a result that is similar to one where liquid viscosity controlled the friction over the whole distance (L. Wilson, personal communication).

The factors which control the dimensions of the conduit are likely to be the regional stress field, magmatic pressure prior to eruption, deformation of the overlying crustal rocks and erosion of the conduit during an eruption. Observations

of many plinian fall deposits suggest that eruptions of this type usually, although certainly not always, are characterized by an increase in intensity during individual events. This is reflected in the reverse size grading of widely dispersed pyroclasts within the fall deposits (Wilson et al. 1980). Carey and Sigurdsson (1987) have inferred that the magma discharge rate (intensity) of the A.D. 79 eruption of Vesuvius changed by over an order of magnitude during the course of the event. Given that the excess pressure within a chamber is likely to fall as magma is withdrawn, the most reasonable explanation for the increase in intensity with time lies in the progressive increase in the diameter of the conduit and vent by erosion. These observation suggest that *initial* dimensions of the conduit may not necessarily be different between eruptions but that the amount of erosion that takes place may ultimately determine the maximum dimension.

We suggest that the ultimate vent and conduit dimensions are likely to be dependent upon the duration of the plinian phase of the eruption. The longer an eruption is sustained the more erosion can take place and the higher the peak intensity will be. The duration of an eruption will depend upon the amount of magma which can be withdrawn from a specific reservoir. Blake (1981) has argued that for a constant volume chamber the amount of magma that is erupted in any particular eruption is given by

$$\frac{\Delta V}{V_c} = \frac{\sigma}{b} \tag{4}$$

where ΔV is the volume of expelled magma, V_c is the volume of the chamber, σ is the tensile strength of the crust, and b is the bulk modulus of the magma. This relation holds for the point at which the magmatic pressure exceeds the tensile strength of the surrounding rocks and failure occurs. The amount of magma that can be erupted is thus proportional to the total volume of the chamber. It is unlikely, however, that the assumption of constant chamber size is realistic considering the many observations that demonstrate inflation prior to volcanism. If the chamber is allowed to expand in volume then the erupted volume is expressed by

$$\frac{\Delta V}{V_c} \approx \frac{\sigma}{b}(1+s)+s \tag{5}$$

where s is the fractional volumetric expansion. The volume of erupted magma is still proportional to the size of the chamber but is also now dependent upon the extent to which it can enlarge to accomodate new magma.

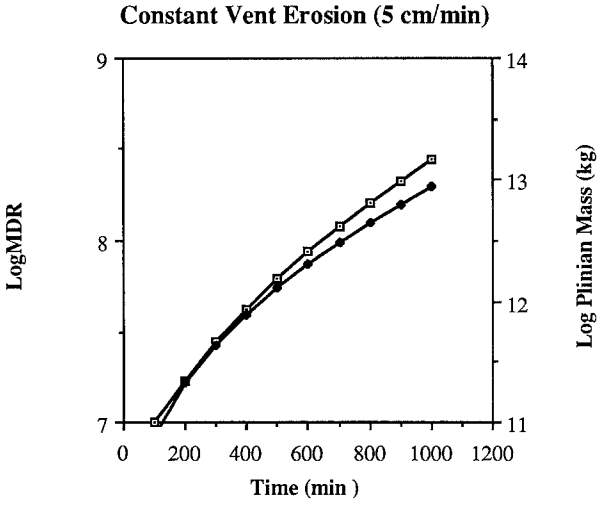

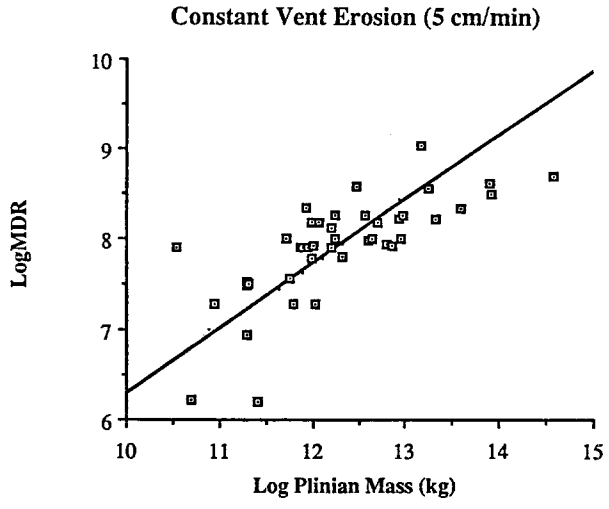

Fig. 4. Variation of magma discharge rate *(solid diamonds)* and total erupted mass *(open boxes)* as a function of time for a hypothetical eruption which begins with a 30 m radius conduit and enlarges at a constant rate of 5 cm/min. Equation (3) in the text was used to calculate the mass eruption rate assuming a difference in density between magma and crustal rocks of 150 kg/m^3 and a magma viscosity of 2.3×10^6 Poise. Total erupted mass was calculated by integrating equation (3) over the appropriate time intervals

Fig. 5. Predicted relationship *(solid line)* between the log of mass eruption rate (intensity) and the log of the total erupted mass *(plinian)* for a constant vent/conduit enlargement of 5 cm/min. *Open squares* are the data for the inferred intensities and plinian masses of the 45 Pleistocene and Recent eruptions

We suggest that the correlation between the peak intensities of plinian fall phases and the total erupted mass (Figs. 2a, b) results primarily from an influence of magma chamber size on the evolution of eruptive processes. Because the volume of magma that can be erupted during an event is proportional to the volume of the source chamber, the potential for erosion and enlargement of conduits and vents is greater for eruptions from large volume reservoirs. Consider the simple case where the radius of the conduit increases at a constant rate during an eruption. The intensity will vary as r^4, from equation 3, whereas the total erupted volume will vary as r^5 because of the need to integrate the variation of intensity as a function of time. Figure 4 shows the variation of intensity and erupted mass as a function of time for a hypothetical eruption with an initial 30 m radius conduit which erodes at a constant rate of 5 cm/min. The strong dependence of intensity on conduit radius (equation 3) allows the three order of magnitude range of intensities to be accounted for by a factor of 6 variation in r. Figure 5 shows the predicted relationship between *peak* intensity and the total erupted mass for a constantly eroding conduit. Superimposed on this trend are the data of inferred intensity and mass of the plinian deposits in our dataset. There is fairly good agreement between the predicted trend and the observational data. We point out that the erosion rate of 5 cm/min is based on the order of magnitude increase in magma discharge rate within the timeframe of the A.D. 79 eruption of Vesuvius (Carey and Sigurdsson 1987). This simple model predicts, of course, that all plinian deposits should exhibit reverse size grading as the intensity is continuously increasing throughout the eruption. Despite the fact that many plinian deposits exhibit this feature there are certainly many examples with either ungraded or even normally graded patterns. In other words, we cannot rule out the possibility that there are differences in the *initial* conduit dimensions of various eruptions and that the rate of vent erosion may indeed not be constant.

An additional factor, as argued above, involves the initial pressure gradient, which is also dependent upon and positively correlated with chamber size (Fig. 3). This effect may act in concert with the total volume discharge to enhance the extent of erosion and enlargement of the conduit and vent. Finally, it is possible that chamber size may influence the initial size of conduits if the release of strain at the inception of eruption is proportional to the total deformation associated with inflation of the reservoir. At present we do not have a suitable model to evaluate this effect but we speculate that it too would serve to enhance the relationship between chamber size and intensity of the plinian phase.

Transitions of eruptive style during plinian eruptions

The idealized stratigraphic sequence of ignimbrite-forming eruptions proposed by Sparks et al. (1973) placed the plinian fall phase at the base, followed by surge and then pyroclastic flow deposits. The transition from fall to flow activity was attributed to the collapse of the plinian column as eruptive conditions changed during the course of the eruption (Sparks and Wilson 1976; Wilson et al. 1980). Conditions which favour the collapse of an eruption column include: (1) increasing intensity at constant magmatic volatile content, or (2) decreasing volatile content at constant intensity (Fig. 6). In our dataset virtually all

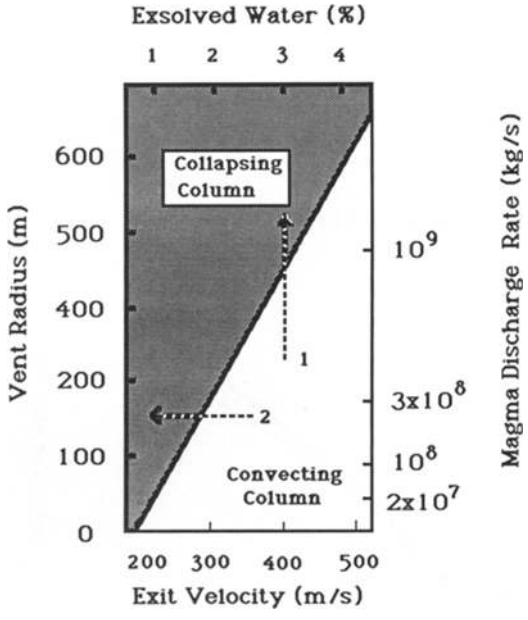

Fig. 6. Relationship between vent radius, magma discharge rate, exsolved magmatic volatiles and exit velocity and their effect on the stability of eruption columns from Wilson et al. (1980). Various combinations of the parameters define two fields of column behaviour: collapsing and convective rise. Transitions from a convecting column to a collapsing column can occur by two different trajectories shown as *dashed lines:* (1) large increases in the intensity or vent size or (2) decrease in volatile content or exit velocity of magma. Caldera-forming events which generate large-volume pyroclastic flows probably follow trajectory *(1)*, whereas small-volume pyroclastic flow generation may occur along trajectories similar to *(2)*

of the eruptions that had intensities exceeding 2×10^8 kg/s were terminated by the generation of large-volume pyroclastic flows. Smaller magnitude eruptions were characterized by more localized intraplinian pyroclastic flows or none at all.

Most of the large-volume ignimbrites were associated with the formation of calderas or downsagged structures (Walker 1984). The difference between these deposits and the intraplinian flows of the smaller magnitude eruptions may reflect a fundamental difference in the way pyroclastic flows are generated in eruptions of different intensity. Recent observations of the 1980 eruptions of Mount St. Helens have shown that small pyroclastic flows can be generated during a roughly continuous plinian phase by short-lived oscillations of eruption column properties which lead to partial collapse (Rowley et al. 1981; Hoblitt 1986). These transitions probably cross the column stability border (Fig. 6) by reduction of volatile content or exit velocity, instead of large increases in intensity. On the other hand, voluminous pyroclastic flows associated with large magnitude, caldera-forming events are likely to be generated by piercing the stability border through large increases in intensity. These eruptions evolve to high intensities due to erosion of the conduit and vent, and allow great quantities of magma to be evacuated in short periods of time. This evacuation, coupled with the pressure drop in the upper part of the chamber, leads to the catastrophic failure of the roof rocks and subsidence into the upper portions of the chamber. This failure results in the establishment of enlarged passageways to the surface and a dynamic pressure on the remaining magma body which produces very high intensity and a transition to collapsing conditions. A direct result of the collapse phase is that a larger fraction of the initial reservoir volume can be expelled than if only compressibility or pre-eruption inflation are considered (Blake 1981). Such a system is rarely able to re-establish the conditions of a convectively rising column.

In many respects this model is similar to that proposed by Druitt and Sparks (1984) or Whitney and Stormer (1986) but now modified to account for the observed variation of plinian intensity by conduit/vent erosion and initial pressure gradients that are dependent on chamber size. We speculate that caldera formation is favoured for volcanic systems with large chambers because the high intensity of the initial plinian phase allows evacuation of large magma volumes in a short period of time. If the elastic rebound of the overlying crustal rocks does not keep pace with magma withdrawal, then catastrophic foundering of the chamber roof results in caldera or downsagged structure formation. Smaller magnitude events evacuate chambers at a slower pace which is simultaneously compensated by smaller amounts of gradual crustal subsidence and lower tendency for the formation of collapse features.

Discussion

The correlation between plinian phase intensity and total eruption magnitude can be, to a first order, predicted by a simple model of conduit/vent erosion coupled with magma overpressure caused by buoyancy. Differences in intensity are attributed to absolute differences in the degree of conduit/vent erosion caused by the duration of the plinian phase, which in turn is related to the fraction of the magma reservoir that can be ejected during a single event. This fraction and the initial pressure gradient is positively correlated with chamber size. It is unlikely, however, that chamber size alone is responsible for the observed distribution of intensity versus magnitude (Fig. 2a, b). For example, at constant intensity or magnitude, the complementary parameter exhibits a range exceeding one order of magnitude in each case. These deviations from the simple intensity/magnitude correlation are probably the result of volatile content and viscosity differences of magmas. More studies are needed before the contribution of each parameter can be rigorously specified.

The correlation between eruption intensity and magnitude has important implications for volcanic hazard assessment. The data suggest that sustained, high intensity plinian phases ($> 2.0 \times 10^8$ kg/s) typically herald the generation of very large volume pyroclastic flows and caldera collapse. Because eruption column height is a direct indicator of eruption intensity, plinian eruption columns could be viewed as a sort of flowmeter on a grand scale. Sustained eruption column heights of 35 km or more should alert observers to the potential of major pyroclastic flow generation. Because these plinian phases last at least several hours, this could provide additional time to evacuate a wide area in anticipation of a particularly violent event. We suggest, therefore, that precise column height observations should be considered in an integrated framework of volcano monitoring techniques, as was accomplished at Mount St. Helens (Harris et al. 1981).

The intensity measurements provided in this study, and the associated correlation, provide a new perspective with which to examine the problem of explosive eruption classification. Fedotov (1985) has proposed an eruption scale that is based solely on intensity. A singular parameter of eruption scale is, however, not appropriate for complex explosive eruption sequences, as pointed out by Walker (1980). Two of the parameters proposed by Walker, intensity and magnitude, can now be quantified for both recent and ancient eruptions. An eruption scale based on these two measurements would provide a more informative numerical description of an eruption. The VEI index of Newhall and Self (1982) is an attempt at combining these parameters, and some others, but the increments of the index are arbitrarily chosen and assume a fixed inter-relationship of the various parameters. In Fig. 7 the subdivisions of the VEI have been superimposed on our intensity/magnitude plot. All of the eruptions in our data set would be classified as VEI index 3 or greater. There are several eruptions, however, which fall outside of the VEI ranges. In particular, there is a cluster of events with column heights in excess of 25 km but with magitudes less than 2.4×10^{12} kg. In the absence of intensity determinations, these eruptions would be classified as VEI 4, despite the fact that they have column heights as high as VEI 5 or 6 events. The current VEI magnitude boundary between index 5 and 6 is very close to a significant natural boundary of eruption types. Eruptions of index 6 or greater are predominantly caldera-forming events which generate major pyroclastic flows.

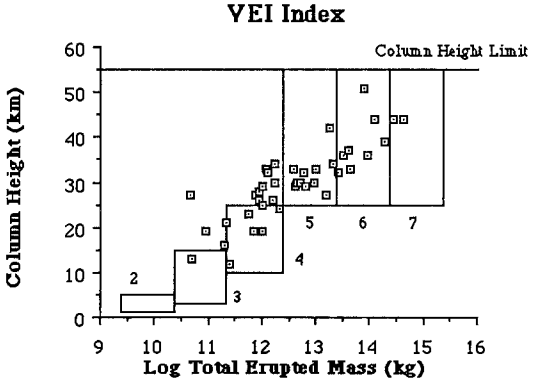

Fig. 7. Plot of eruption column height versus log of the total erupted mass for Pleistocene and Recent plinian deposits. Intensity and magnitude boundaries of the Volcanic Explosivity Index (VEI) from 2 to 7 are shown as a series of *rectangles*. Note that many of the eruptions fall outside of the current VEI boundaries

Our analysis shows that although intensity and magnitude are correlated, a wide range of magnitude exists amongst eruptions of similar intensity. Rather than adopt a simple scale for volcanic activity, we feel that both intensity and magnitude should be stated wherever possible.

Conclusions

Modelling of pyroclast fallout shows that 45 plinian eruptions of Pleistocene and Recent age varied in intensity (rate of magma discharge) by three orders of magnitude from 1.6×10^6 kg/s to 1.1×10^9 kg/s. The magnitudes of these same eruptions, or the total mass of erupted material, also varied over three orders of magnitude from 2×10^{11} kg/s to 6.8×10^{14} kg/s. A positive correlation is found between the intensity of the plinian fall phase and the magnitude of the entire eruption (pyroclastic flows and surges included). This is primarily attributed to differences in the degree to which conduits/vents are enlarged during explosive eruptions by erosion. We suggest that the extent of the conduit enlargement is a function of the amount of magma expelled during the plinian phase and is thus proportional to the total reservoir volume based on considerations of the behaviour of open magmatic systems by Blake (1981). Chamber size also plays a role in determining the initial presure gradient which drives magma out of the chamber to the surface. The effect is, however, a monotonic rise in pressure gradient as the vertical extent is increased. Other factors, such as magmatic volatile content and viscosity are likely to affect the primary correlation in complex ways that blur, but do not obscure, the overall effect of reservoir size.

The wide spectrum of eruption magnitudes and intensities suggest at least two different ways in which the style of plinian eruptions undergo transitions to pyroclastic flow generation. Using theoretical models of column collapse by Sparks et al. (1978) and Wilson et al. (1980) as a frame of reference, transitions from a convecting to a collapsing column are likely to occur by either reduction of magmatic volatile content or large increases in intensity. We speculate that the former is typical of small and intermediate intensity plinian eruptions whereas the latter is characteristic of high intensity, caldera-forming events.

This study illustrates the potential of sustained eruption column height as an indicator of ultimate eruption magnitude and style. We therefore believe that column height is an important param-

eter to monitor in programs designed for volcanic hazard assessment because of its predictive potential for the evolutionary sequence of plinian eruptions.

Acknowledgments. This work has been supported by grants from the National Science Foundation (EAR-8416782 and EAR-8306384) and the National Geographic Society. We thank Winton Cornell and Robert Detrick for useful discussions on various aspects of this work. Stephen Sparks's contribution to the fallout modelling and other treatments of plume dynamics were instrumental to the analysis of the intensity of plinian eruptions. Lionel Wilson provided many useful comments particularly regarding the role of conduit dimensions in controlling eruption intensity. Two anonymous reviewers made numerous suggestions which significant improved the text.

References

Aramaki S (1984) Formation of the Aira Caldera, Southern Kyushu, ~22,000 years ago. J Geophys Res 89:8485–8501

Blake S (1981) Volcanism and the dynamics of open magma chambers. Nature 289:783–785

Bloomfield K, Rubio G, Wilson L (1977) Plinian eruptions of Nevado de Toluca volcano, Mexico. Geol Rund 66:120–146

Bond A, Sparks RSJ (1976) The Minoan eruption of Santorini, Greece. J Geol Soc Lond 132:1–16

Carey S, Sigurdsson H (1985) The May 18 eruption of Mount St. Helens 2. Modelling of dynamics of the plinian phase. J Geophys Res 90:2948–2958

Carey S, Sigurdsson H (1986) The 1982 eruptions of El Chichon volcano, Mexico (2): Observations and numerical modelling of tephra fall distribution. Bull Volcanol 48:127–141

Carey S, Sigurdsson H (1987) Temporal variations of column height and magma discharge rate during the 79 AD eruption of Vesuvius. Bull Geol Soc Amer 99:303–314

Carey S, Sparks RSJ (1986) Quantitative models of fallout and dispersal of tephra from volcanic eruption columns. Bull Volcanol 48:109–125

Cornell W, Carey S, Sigurdsson H (1983) Computer simulation of transport and deposition of the Campanian Y-5 ash. J Volcanol Geotherm Res 17:89–109

Druitt T, Sparks RSJ (1984) On the formation of calderas during ignimbrite eruptions. Nature 310:679–681

Elder JW (1979a) Magma traps: Part I, Theory. J Pure Appl Geophys 117:3–14

Elder JW (1979b) Magma traps: Part II, Application. J Pure Appl Geophys 117:15–33

Fedotov SA (1985) Estimates of heat and pyroclast discharge by volcanic eruptions based upon the eruption cloud and steady plume observations. J Geodynam 3:275–302

Fierstein J, Hildreth W (1986) Ejecta dispersal and dynamics of the 1912 eruptions at Novarupta, Katmai National Park, Alaska. EOS Trans Am Geophys Union 67(44):1246

Gorshkov GS (1959) Gigantic eruption of the volcano Bezymianny. Bull Volcanol 20:77–109

Harris D, Rose WI, Roe R, Thompson M (1981) Radar observation of ash eruptions. US Geol Surv Prof Pap 1250:323–334

Hayakawa Y (1985) Pyroclastic geology of Towada Volcano. Bull Earth Res Instit Univ Tokyo 60:507–592

Hoblitt RP (1986) Observations of the eruptions of July 22 and August 7, 1980 at Mount St. Helens, Washington. US Geol Surv Prof Pap 1335:1–44

Katsui Y (1959) On the Shikotsu Pumice-fall Deposit, Special Reference to the Activity just before the Depression of the Shikotsu Caldera. Bull Volcanol Soc Japan 4(2):33–48

Kobayashi T, Hayakawa Y, Aramaki S (1983) Thickness and grain-size distribution of the Osumi pumice fall deposit from the Aira caldera. Bull Volcanol Soc Japan 28(2): 129–139

Lirer L, Pescatore T, Booth B, Walker GPL (1973) Two plinian pumice-fall deposits from Somma Vesuvius, Italy. Bull Geol Soc Am 84:759–772

Naranjo J, Sigurdsson H, Carey S, Fritz W (1986) Eruption of Nevado del Ruiz, Colombia, on 13 November 1985: Tephra fall and lahars. Science 233:961–963

Newhall C, Self S (1982) The volcanic explosivity index (VEI): an estimate of explosive magnitude for historical volcanism. J Geophys Res 87:1231–1238

Pescatore T, Sparks RSJ, Brazier S (1987) Reverse grading in the Avellino plinian deposit of Vesuvius. Bull Volcanol (in press)

Pollard D, Muller O (1976) Effect of gradients in regional stress and magma pressure on the form of sheet intrusions in cross section. J Geophys Res 81:975–984

Robson G, Barr K (1964) The effect of stress on faulting and minor intrusions in the vicinity of a magma body. Bull Volcanol 27:315–330

Rose WI, Newhall C, Bornhorst T, Self S (1987) Quaternary silicic pyroclastic deposits of Atitlan caldera, Guatemala. J Volcanol Geotherm Res 33:57–80

Rowley P, Kuntz M, Macleod N (1981) Pyroclastic flow deposits: The 1980 eruptions of Mount St. Helens, Washington. US Geol Surv Prof Pap 1250:489–512

Settle M (1978) Volcanic eruption clouds and the thermal power output of explosive eruptions. J Volcanol Geotherm Res 3:309–324

Shaw HR (1980) The fracture mechanisms of magma transport from the mantle to the surface. In: Hargraves RB (ed) Physics of magmatic processes, pp 201–232

Sigurdsson H, Carey S, Cornell W, Pescatore T (1985) The eruption of Vesuvius in A.D. 79. Nat Geograph Res 1(3):332–387

Sigurdsson H, Carey S (1989) The 1815 eruptions of Tambora, Indonesia: generation of co-ignimbrite ash fall during entrance of pyroclastic flows into the ocean. Bull Volcanol 51 (in press)

Sparks RSJ (1986) The dimensions and dynamics of volcanic eruption columns. Bull Volcanol 48:3–15

Sparks RSJ, Wilson L (1976) A model for the formation of ignimbrite by gravitational column collapse. J Geol Soc Lond 132:441–451

Sparks RSJ, Self S, Walker GPL (1973) Products of ignimbrite eruptions. Geology 1:115–118

Sparks RSJ, Wilson L, Hulme G (1978) Theoretical modeling of the generation, movement, and emplacement of pyroclastic flows by column collapse. J Geophys Res 83:1727–1739

Sparks RSJ, Wilson L, Sigurdsson H (1981) The pyroclastic deposits of the 1875 Askja eruption, Iceland. Phil Trans Roy Soc Lond 29:241–273

Sparks RSJ, Moore JG, Rice CJ (1986) The initial giant eruption cloud of the May 18, 1980, explosive eruption of Mount St. Helens. J Volcanol Geotherm Res 28:257–274

Sussman D (1985) Apoyo caldera, Nicaragua: a major Quaternary silicic eruptive center. J Volcanol Geotherm Res 24:249–282

Traineau H, Westercamp, D (1985) Les éruptions ponceuses récentes de la Montagne Pelée (Martinique) Description des dépôts-dynamique éruptifs. IMRG A.F.M.E. 85 SGN 471 IRG:1–68

Walker GPL (1980) The Taupo pumice: products of the most powerful known (ultraplinian) eruption? J Volcanol Geotherm Res 8:69–94

Walker GPL (1981a) Plinian eruptions and their products. Bull Volcanol 44-2:223–240

Walker GPL (1981b) The Waimihia and Hatepe plinian deposits from the rhyolitic Taupo volcanic center. New Zeal J Geol Geophys 24:305–324

Walker GPL (1984) Downsag calderas, ring faults, caldera sizes, and incremental caldera growth. J Geophys Res 89:8407–8416

Walker GPL, Croasdale R (1973) Two plinian-type eruptions in the Azores. J Geol Soc Lond 127:17–55

Walker GPL, Wright JV, Clough BJ, Booth B (1981) Pyroclastic geology of the rhyolitic volcano of La Primavera, Mexico. Geol Rundsch 70:1100–1118

Walker GPL, Self S, Wilson L (1984) Tarawera 1886, New Zealand- a basaltic plinian fissure eruption. J Volcanol Geotherm Res 21:61–78

Watkins ND, Sparks RSJ, Sigurdsson H, Huang TC, Federman A, Carey S, Ninkovich D (1978) Volume and extent of the Minoan tephra from Santorini Volcano: new evidence from deep-sea cores. Nature 271:122–126

Weertman J (1971) Theory of water-filled crevasses in glaciers applied to vertical magma transport beneath oceanic ridges. J Geophys Res 76:1171–1183

Whitney J, Stormer JC Jr (1986) Model for the intrusion of batholiths associated with the eruption of large volume ash flow tuffs. Science 231:483–485

Williams SN, Self S (1983) The October, 1902 plinian eruption of Santa Maria volcano, Guatemala. J Volcanol Geotherm Res 16:33–56

Wilson L (1980) Relationships between pressure, volatile content and ejecta velocity in three types of volcanic explosions. J Volcanol Geotherm Res 8:297–313

Wilson L, Head J (1981) Ascent and eruption of basaltic magma on the Earth and Moon. J Geophys Res 86:2971–3001

Wilson CJN, Walker GPL (1985) The Taupo eruption, New Zealand I. General aspects. Phil Trans Roy Soc Lond A 314:199–228

Wilson L, Sparks RSJ, Huang TC, Watkins ND (1978) The control of volcanic column heights by eruption energetics and dynamics. J Geophys Res 83:1829–1836

Wilson L, Sparks RSJ, Walker GPL (1980) Explosive volcanic eruptions IV. The control of magma properties and conduit geometry on eruption column behaviour. Geophys J Roy Astrom Soc 63:117–148

Wright JV (1981) The Rio Caliente ignimbrite: analysis of a compound intraplinian ignimbrite from a major late Quaternary Mexican eruption. Bull Volcanol 44-2:189–212

Received April 22, 1987/Accepted May 4, 1988